Ionic Currents in the Human Serotonin Transporter Reveal Inconsistencies in the Alternating Access Hypothesis

Scott V. Adams* and Louis J. DeFelice†
*Department of Physics and Astronomy and †Department of Pharmacology, Vanderbilt University, Nashville, Tennessee 37232

ABSTRACT We have investigated the conduction states of human serotonin transporter (hSERT) using the voltage clamp, cut-open frog oocyte method under different internal and external ionic conditions. Our data indicate discrepancies in the alternating access model of cotransport, which cannot consistently explain substrate transport and electrophysiological data. We are able simultaneously to isolate distinct external and internal binding sites for substrate, which exert different effects upon currents conducted by hSERT, in contradiction to the alternating access model. External binding sites of coupled Na ions are likewise simultaneously accessible from the internal and external face. Although Na and Cl are putatively cotransported, they have opposite effects on the internal face of the transporter. Finally, the internal K ion does not compete with internal 5-hydroxytryptamine for empty transporters. These data can be explained more readily in the language of ion channels, rather than carrier models distinguished by alternating access mechanisms: in a channel model of coupled transport, the currents represent different states of the same permeation path through hSERT and coupling occurs in a common pore.

INTRODUCTION

The human serotonin transporter (hSERT) couples the movement of serotonin (5-hydroxytryptamine, 5HT) and other ions, typified by Na, across the plasma membrane. By a poorly understood mechanism, hSERT utilizes the energy stored in transmembrane ionic gradients to establish a 5HT gradient. This type of transport is referred to as secondary transport, in contrast to the primary transport coupling through ATPases, which establish the ionic gradients used by hSERT (Läuger, 1991). Clearing extracellular 5HT is the primary physiological function of hSERT, both in the central nervous system (Iversen, 1971; Ramamoorthy et al., 1993; Bunin and Wightman, 1998) and peripheral tissues such as lung, blood, and the gastrointestinal tract (Ramamoorthy et al., 1993; Eddahibi et al., 2001; Rudnick, 1977; Chen et al., 2001). Control of extracellular 5HT levels is important because of the widespread distribution and abundance of 5HT receptors. Thus, in diverse physiological contexts, SERT functions to regulate serotonergic signaling. Coupling is a critical feature of SERT function, because SERT is capable of clearing 5HT even when internal [5HT] exceeds external [5HT].

Radiolabeled tracer flux studies have long been the standard technique employed to study transport and coupling in SERT (Rudnick, 1998). Often, to explain transport data these studies focus on the ''alternating access'' hypothesis, in which binding sites on hSERT for 5HT and ions alternately face extracellular or cytoplasmic compartments. Within this framework, coupling results from conformational changes in the transporter induced by substrate and ion binding (Jardetsky, 1966). Flux experiments have resulted in a widely accepted electroneutral scheme for SERT in which Na, Cl, and 5HT are cotransported, and K or H is countertransported (Nelson and Rudnick, 1979; Rudnick and Clark, 1993; Gu et al., 1994, 1996).

However, a second possible mechanism for coupled cotransport, also supported by tracer flux data (Adams and DeFelice, 2002), as well as electrophysiological data (Galli et al., 1996, 1997, 1998; Petersen and DeFelice, 1999), postulates that substrate and ions share a complex pore. In this scenario, coupling occurs as a result of interactions between substrate and ion in the pore lumen, referred to as flux coupling (for related theories and applications, see Hodgkin and Keynes, 1955; Su et al., 1996; Chou, 1999; Chou and Lohse, 1999; DeFelice and Adams, 2001; DeFelice et al., 2001). A simplified example of coupling in a single-file, knock-through channel, in which Na ions moving down their electrochemical gradient and push 5HT up its gradient appears in Adams and DeFelice (2002).

In addition to transporting 5HT, SERT conducts several different ionic currents, both steady state and transient (Mager et al., 1994; Li et al., 2002). Steady-state substrate-induced currents have been observed in many members of the Na/Cl-dependent GAT/NET gene family (Mager et al., 1994; Sonders et al., 1997; Mager et al., 1993; Sonders and Amara, 1996). For the monoamine transporters (i.e., 5HT, dopamine, and norepinephrine transporters) this current is loosely termed ''uncoupled'' because it greatly exceeds the current predicted from measurements of the expression level, turnover rate, and net charged moved per coupled transporter cycle according to putative alternating access schemes (Blakely et al., 1994; Galli et al., 1996; Mager et al., 1994; Sonders et al., 1997). In addition to substrate-induced currents, monoamine transporters are reported to conduct substrate independent (leak) current (Mager et al., 1994; Sonders et al., 1997), as well as currents induced by external Li (Mager et al., 1994), acidic pH (Cao et al., 1997, 1998),

Submitted January 14, 2003, and accepted for publication May 21, 2003.
Address reprint requests to Louis J. DeFelice, Dept. of Pharmacology, Center for Molecular Neuroscience, Vanderbilt University Medical Center, Nashville, TN 37232-8548. Tel.: 615-343-6278; Fax: 615-343-1679; E-mail: lou.defelice@vanderbilt.edu.

0006-3495/03/09/1548/12 $2.00

psychostimulants (Mager et al., 1994; Sonders et al., 1997), or second messengers (Ingram and Amara, 2000).

In this article, we employ the cut-open *Xenopus* oocyte voltage clamp (COVC) technique to measure ionic currents conducted by hSERT. COVC (Stefani and Bezanilla, 1998; Kaneko et al., 1998; Costa et al., 1994) allows simultaneous, dynamic access to the internal and external face of the transporter, so that interactions between substrate, ions, and hSERT may be probed in detail. Ionic current through transporters is an assay for transporter conformation, whether or not the current itself represents 5HT transport. Thus we can use ionic currents to test functional models, such as the alternating access model, which postulate specific relationships between SERT conformational states. This method has revealed inconsistencies in the alternating access model of transporter function.

MATERIALS AND METHODS

Oocyte harvest, culture, and preparation

Oocytes were surgically removed from mature *Xenopus laevis* anaesthetized with 0.2% tricaine. Surgery was performed aseptically and in compliance with Vanderbilt University regulations. After removal from the frog, the follicular tissue containing the oocytes was placed in Ringer's buffer (R96 (mM): 96 NaCl, 2 KCl, 5 $MgCl_2$, 5 HEPES) with 10 μg/mL gentamicin, and gently cut into small pieces. Aliquots of this tissue (3–4 mL each) were added to 10 mL R96 with 0.2% collagenase, and nutated for 90–110 min. Collagenase treatment was terminated by repeated washing in R96 + 0.6 mM $CaCl_2$ (R96 + Ca) when visual inspection of the oocytes revealed that the majority of the oocytes were not surrounded by follicular tissue. We selected stage V-VI oocytes for cRNA injection within 24 h of oocyte isolation. cRNA was transcribed from cDNA in the pOTV vector (gift of Dr. M. Sonders, Vollum Institute), using Ambion mMessage Machine T7 kit (Ambion, Austin, TX). Each oocyte was injected with 23 ng cRNA and incubated at room temperature (23 ± 3°C) for 4–8 days, in R96+Ca supplemented with 550 μg/mL NaPyruvate, 100 μg/mL streptomycin, 50 μg/mL tetracycline, and 5% dialyzed horse serum (Elsner et al., 2000; Quick et al., 1992; Goldin, 1992; Stuhmer, 1998).

Electrophysiology

We employed the cut-open oocyte voltage clamp recording technique (Stefani and Bezanilla, 1998; Kaneko et al., 1998) as modified by Costa et al. (1994). Originally designed for application to voltage-activated ion channels, COVC has been applied previously to the glucose cotransporter SGLT1 (Chen et al., 1995, 1996) and the amino-acid exchanger rBAT (Coady et al., 1994, 1996). This technique allows reproducible manipulation of the internal and external ionic environment of the oocyte (see Fig. 1 *A*). *N*-methyl-D-glucamine (NMDG) replaced cations and methanesulfonate (MES) replaced Cl as described for individual experiments (see Results below). Internal Oocyte Buffer (IOB (mM): 50 KCl, 70 K-MES, 5 Na-MES, 10 HEPES, 2 $MgCl_2$, 0.5 EGTA, 0.1 ascorbic acid, 0.1 pargyline; pH 7.4 with NMDG-OH) was perfused at 10–30 μL/min. Total osmolarity, and final pH of all solutions, was always verified to ensure consistency. We found that completely changing the internal ionic concentration took 5–30 min, depending upon pipette diameter and its distance from the internal face of the membrane. Therefore, we performed only one such solution change per oocyte, pairing the experimental condition to a standard baseline. For at least one oocyte in each experimental internal solution, we were able to return the internal solution to the baseline solution, demonstrating that the effects of internally applied ions and substrate are reversible. External solution (R96ext) consisting of R96+Ca, with additional 0.1 mM ascorbic acid and 0.1 mM pargyline, was applied to the oocyte at ~1 mL/min through a movable, sawed-off 18-gauge syringe placed near the oocyte dome. External solution change was therefore rapid. Reported data report only currents that are activated by external application of 5HT, DS, or Li that washed out (to 10%) upon return to R96ext solution. Typically, each experiment (a single oocyte) lasted 60–90 min. In our apparatus, the agar bridges (1–2% agarose, 120 mM Na-MES, 10 mM HEPES, pH 7.4 with NaOH) connected the solution baths to wells filled with 1 M NaCl and Ag/AgCl pellets, relaying electrophysiological currents to the amplifier (Dagan, Minneapolis, MN). Voltage protocols were applied using AxoClamp 7.0 software (Axon Instruments, Union City, CA) on a desktop PC. Data were filtered at 1 kHz by the amplifier, and digitized at 2 kHz by the acquisition software. In most experiments, we partially compensated the membrane transients to speed the membrane voltage clamp. External solutions were controlled with electronic values and pressurized reservoirs set to 1 PSI (Automate Scientific, San Francisco, CA).

Data analysis

Subtracted electrophysiological currents are shown, except in the raw traces in Fig. 1, *B–D*. Subtraction was performed after averaging each trace over the last 25 ms of each potential step, and was defined as I (presence of activator) − I (R96ext), for 5HT-induced current (I_{5HT}), Li-induced current (I_{Li}), and desipramine (DS)-revealed current (I_{Leak}). For I_{Leak}, the subtraction procedure results in a signature negative slope conductance (Mager et al., 1994). Subtracted currents are normalized to the most hyperpolarized potential value (−80 or −100 mV) for each oocyte. This allows for comparison and pooling among many oocytes with differing expression levels. Error bars on data plots represent the standard error of the normalized means of 3–6 oocytes.

RESULTS

Internal 5HT inhibits I_{5HT} and I_{Li} but not I_{Leak}

Although many previous studies have examined the properties of ionic currents mediated by SERT when external 5HT is applied (I_{5HT}) (Mager et al., 1994; Cao et al., 1997, 1998; Petersen and DeFelice, 1999; Ramsey and DeFelice, 2002), little is known about the effect of internal 5HT. Fig. 1 *A* shows a diagram of the cut-open voltage clamp setup. Because exchange of the internal milieu is relatively slow in COVC, 5HT could not be acutely applied to the internal face of hSERT. Rather, the current evoked by $5HT_{out}$ was measured in different levels of $5HT_{in}$. The voltage protocol was either single pulses to the test potential (separated by 1 s) or the staircase protocol displayed in Fig. 1, *B–D*. The two protocols gave the same results. As shown in Fig. 1 *B*, application of $[5HT]_{out} = 15\ \mu M$ induced an inward current at test potentials between −100 mV and +20 mV, compared to the background current measured in the absence of $5HT_{out}$. Fig. 2 *A* plots I_{5HT} as a function of the membrane potential for each $[5HT]_{in}$ tested. Every test $[5HT]_{in}$ was paired to a control at $[5HT]_{in} = 0$ in the same oocyte and normalized at −80 mV. At hyperpolarized potentials, internal 5HT inhibits I_{5HT}. At depolarized potentials, however, $5HT_{in}$ does not significantly inhibit I_{5HT}. We also determined that elevating $[5HT]_{in}$ increases the potency of

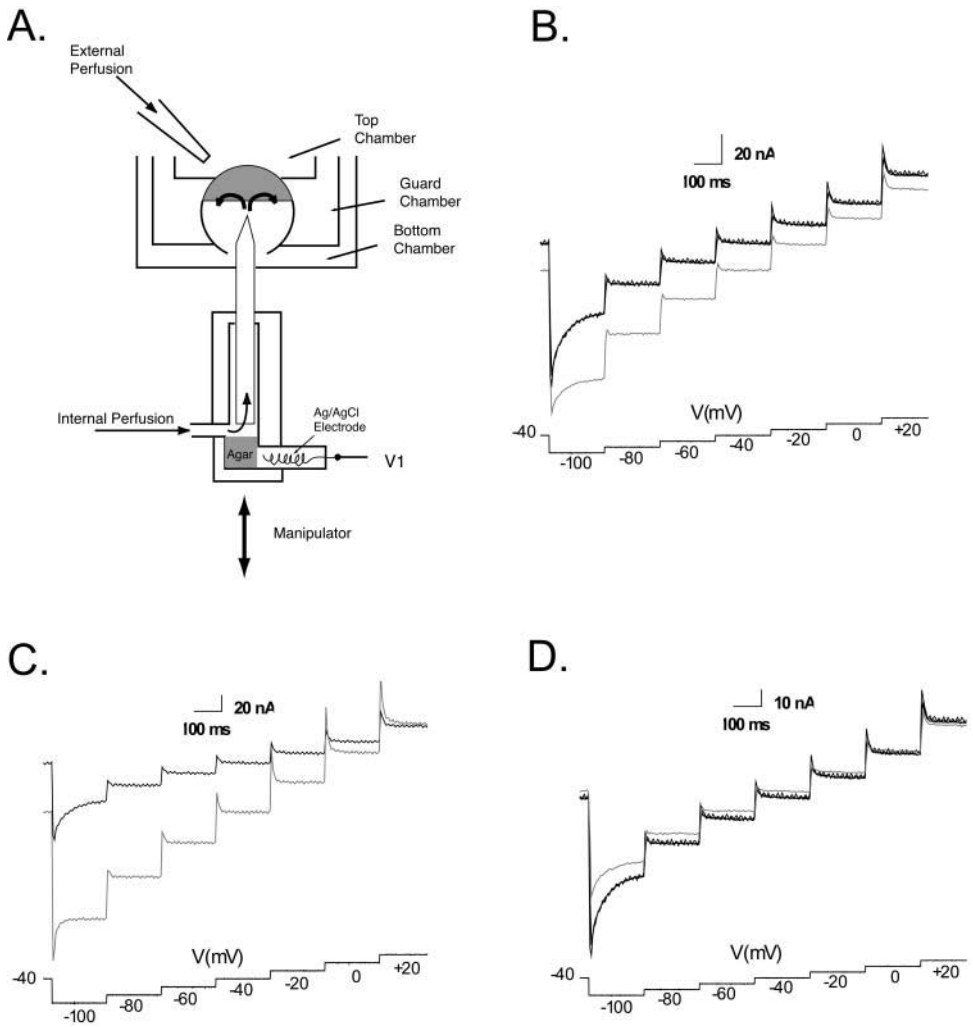

FIGURE 1 Raw current traces from a typical oocyte expressing hSERT. In each panel, the upper (*dark*) trace shows the current before adding the test reagent or exchanging solution, and the gray line shows the response. The lowermost trace shows the voltage protocol. The difference between the steady-state current (*dark*) and test current (*gray*) defines the 5HT (I_{5HT}), Li (I_{Li}), and leak (I_{Leak}) currents. The transitory current, visible at the beginning of each response to a voltage step, is a combination of presteady state and capacitance transient currents. (*A*) Schematic of the cut-open oocyte preparation. The top and bottom chambers are amenable to perfusion and set voltage; the guard chamber isolates the top and bottom chambers. Exposed membrane represents ~10% of the total oocyte membrane. (*B*) Current evoked by application of 15 μM external 5HT. (*C*) Current evoked by complete exchange of external Na with Li. (*D*) Current revealed by application of 2 μM external desipramine.

$[5HT]_{out}$ to elicit I_{5HT}, as shown in Table 1. In each case, the I_{5HT} elicited by varying $[5HT]_{out}$ was fit to $I_{5HT} = I_{max}[5HT]_{out}/(EC_{50} + [5HT]_{out})$. We additionally measured hSERT-mediated currents evoked by the substitution of Li ions for Na ions in the external buffer (I_{Li}) (Fig. 2 *B*). Li-induced current is also inhibited by internal 5HT, with approximately the same potency as I_{5HT}. However, the efficacy of $[5HT]_{in}$ was lower, as maximal $[5HT]_{in} = 1$ mM inhibited the Li current by >50% (Fig. 2 *A*). Previous studies of SERT (Petersen and DeFelice, 1999; Mager et al., 1994) show that $5HT_{out}$ blocks I_{Li}. Finally, we measured the effect of $[5HT]_{in}$ on the constitutive leak current mediated by hSERT, I_{Leak}, by applying 2 μM DS, an hSERT antagonist. Previous experiments showed that 2 μM DS represents a saturating dose of DS ($IC_{50} = 0.49 \pm 0.08$ μM; $n = 1.5 \pm 0.25$; data not shown). Fig. 2 *C* shows that the constitutive leak current is insensitive to $[5HT]_{in}$. Uninjected oocytes showed no response to external 5HT or internal 5HT, a small outward (at −40 mV) response to external Li, and no response to external DS (data not shown). Fig. 2 *D* shows $5HT_{in}$ inhibition of I_{5HT} and I_{Li} at −80 mV. For I_{5HT} the solid line is fit to the equation: $I = 1/(1 + [5HT]_{in}/IC_{50})$, with $IC_{50} = 99 \pm 26$ μM. For I_{Li}, the solid line is drawn by eye, because this equation produced unsatisfactory fit parameters. Both curves are normalized to 1.0 at 0 $5HT_{in}$.

Internal Na inhibits I_{5HT} but not I_{Li}

Next we investigated the interaction of Na with the cytosolic face of the hSERT (Fig. 3). Standard IOB has 5 mM Na and 120 mM K, similar to the native Na content of the oocyte (Dascal, 1987). To reduce complications due to simultaneously lowering $[K]_{in}$ and elevating $[Na]_{in}$, we set $[K]_{in} = 50$ mM as the baseline for experiments with elevated $[Na]_{in}$. As $[Na]_{in}$ increased, we noted a sharp increase in conductance in the oocyte at depolarized potentials. We observed identical behavior in uninjected oocytes (data not shown), but did not attempt to discover the mechanism responsible. Instead, we simply waited for background currents, I_{5HT}, and I_{Li} to stabilize as $[Na]_{in}$ was altered. The results (Fig. 3 *A*) show that $[Na]_{in}$ potently inhibits I_{5HT}, with $IC_{50} \ll 25$ mM and with maximal

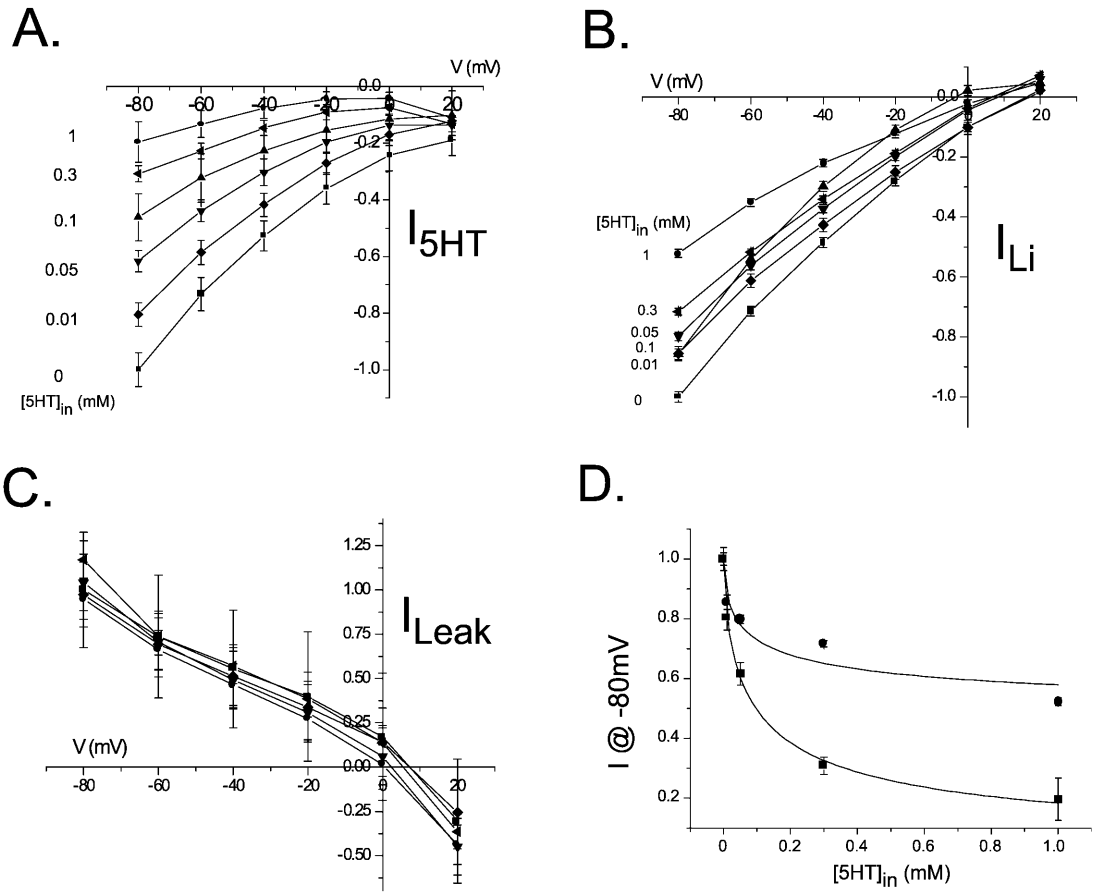

FIGURE 2 Effect of $5HT_{in}$ on hSERT currents. Plotting the steady-state current (I) as a function of the test voltage (V) defines the $I(V)$ characteristic for hSERT (see Fig. 1 for details). (*A*) $I(V)$ showing dose-dependent inhibition of I_{5HT} by $5HT_{in}$. I_{5HT} is elicited with $[5HT]_{out} = 15\ \mu M$. (*B*) $I(V)$ showing inhibition of I_{Li} by $5HT_{in}$. I_{Li} is activated by total replacement of Na_{out} with Li. $5HT_{in}$ doses are represented by same symbols as in *A*. (*C*) $I(V)$ showing lack of effect of $5HT_{in}$ on I_{Leak}. I_{Leak} elicited by $DS_{out} = 2\ \mu M$. $5HT_{in}$ doses are represented by same symbols as in *A*. (*D*) Average inhibition of I_{5HT} (*squares*) ($5HT_{out} = 15\ \mu M$) and I_{Li} (*circles*) at -80 mV. Solid lines are fits to the logistic equation $I = 1/(1 + [5HT]_{in}/IC_{50})$; with $IC_{50} = 99 \pm 26\ \mu M$, the fitting algorithm generates the uncertainty and the IC_{50} applies to both curves normalized to 1.0 at 0 $5HT_{in}$.

efficacy approaching 100%. Surprisingly, $[Na]_{in}$ has only a weak effect on I_{Li} (Fig. 3 *B*). In sharp contrast, $[Na]_{in}$ alters I_{Leak} (Fig. 3 *C*), shifting the reversal potential from +20 mV to −30 mV, consistent with Na permeation contributing to I_{Leak}. However, the apparent outward current at −100 mV is unchanged.

TABLE 1 Internal substrate and ions alter the potency of external 5HT in eliciting I_{5HT} from hSERT

Internal condition	EC_{50} (μM)
$[5HT]_{in}$ (μM)	
0	3.85 ± 0.08
1000	0.86 ± 0.19
$[K]_{in}$ (mM)	
0	0.69 ± 0.36
120	3.25 ± 1.03
$[Cl]_{in}$ (mM)	
0	1.94 ± 0.42
50	1.68 ± 0.51
120	1.23 ± 0.42

For each oocyte, data were fit to a hyperbola, $I = I_{max}[5HT]_{out}/(EC_{50} + [5HT]_{out})$ for the indicated internal ionic condition. These are the average of the fit parameter EC_{50}, ± the standard deviation of the fit values.

Internal Na enhances the effect of internal 5HT

We next checked whether the effects of $[Na]_{in}$ and $[5HT]_{in}$ are independent. For this experiment (Fig. 4), $[Na]_{in}$ was increased to 25 mM, and hSERT currents measured. We then introduced 5HT to the internal solution. Comparison of Fig. 4 *A* with Fig. 2 *A* reveals that increasing $[Na]_{in}$ changes the effect of $[5HT]_{in}$ on I_{5HT}, compared to its effect in low (5 mM) $[Na]_{in}$. With $[Na]_{in} = 25$ mM and $[5HT]_{in} = 1$ mM, I_{5HT} is outward at hyperpolarized potentials and reverses near $V = 0$. This current has the negative-slope conductance characteristic of I_{Leak} under the same experimental conditions (Fig. 4 *C*). Fig. 4 *B* shows that elevated $[5HT]_{in}$ inhibits I_{Li} in the presence of elevated $[Na]_{in}$, consistent with Figs. 2 *B* and 3 *B*. Finally, although I_{Leak} is altered by $[Na]_{in}$, Fig. 4 *C* shows that the altered I_{Leak} remains insensitive to the presence of internal 5HT.

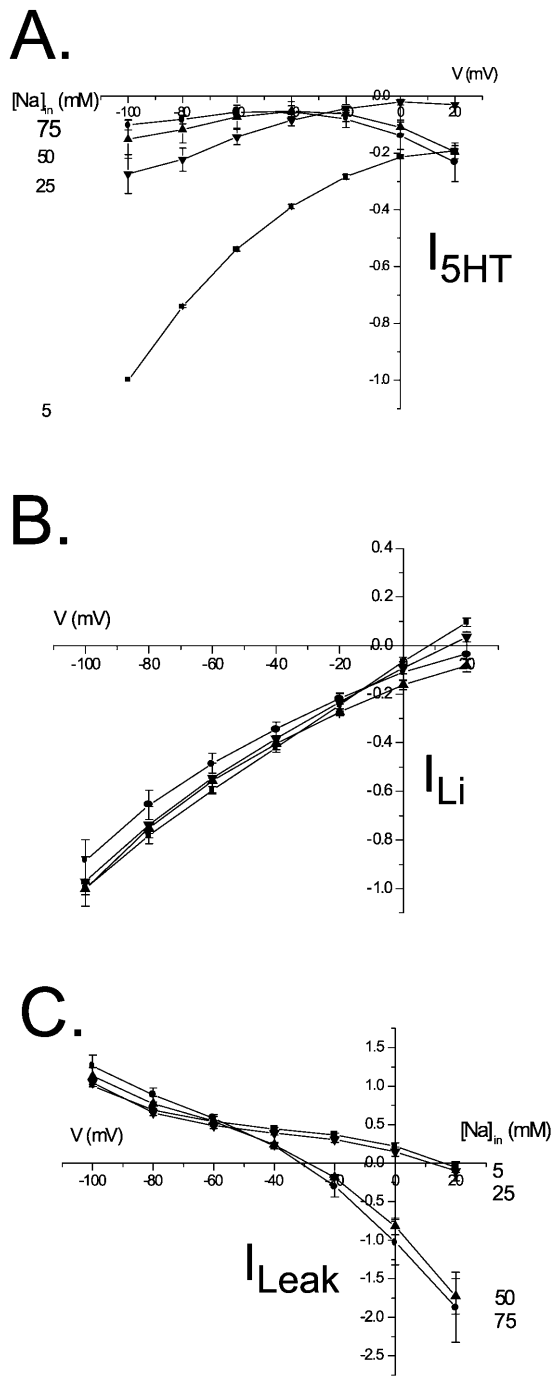

FIGURE 3 Effect of Na_{in} on hSERT currents. Steady-state current (Fig. 1) as a function of the test voltage defines $I(V)$ plots. (*A*) $I(V)$ showing dose-dependent inhibition of I_{5HT} ($[5HT]_{out} = 15\ \mu M$) by Na_{in}. (*B*) I_{Li} $I(V)$ with varied $[Na]_{in}$. Symbols are the same as in *A*. $[Na]_{in}$ has no effect upon I_{Li}. (*C*) The reversal potential of I_{Leak} changes with $[Na]_{in}$.

Internal K potentiates I_{5HT} and I_{Li} but not I_{Leak}

We next explore the effect of putatively countertransported K, by replacing internal K with NMDG. The effect of reducing $[K]_{in}$ from 120 mM to 0 mM is to inhibit I_{5HT} by 60% at −80 mV (Fig. 5 *A*). The EC_{50} for internal K is ~40 mM (Fig. 5 *A*). Similar to I_{5HT}, I_{Li} (Fig. 5 *B*) is decreased by reducing $[K]_{in}$, with EC_{50} ~40 mM, and maximal efficacy ~60% at −80 mV. The leak current revealed by DS application appears insensitive to $[K]_{in}$ (Fig. 5 *C*). Finally, reducing $[K]_{in}$ also increased the potency of external 5HT, as demonstrated by a decreased EC_{50} for external 5HT to elicit I_{5HT} (Table 1).

Internal 5HT inhibits I_{5HT} and I_{Li} in the absence of internal K

To assess the possible interdependence of internal 5HT and internal K we perfuse the cytosol with K-free IOB until obtaining a stable response to external 5HT and external Li. During this stabilization period we observe a steady decrease in evoked currents, consistent with Fig. 5, since the oocyte begins with $[K]_{in}$ ~120 mM. After reaching $[K]_{in} = 0$, we record I_{5HT}, I_{Li}, and I_{Leak}, then exchange the internal solution so that it contains $[5HT]_{in}$ as indicated in Fig. 6. Fig. 6 *A* shows that even with $[K]_{in} = 0$ mM, $[5HT]_{in}$ completely inhibits I_{5HT}, with $IC_{50} = 91 \pm 21\ \mu M$. This value is indistinguishable from the IC_{50} obtained with $[K]_{in} = 120$ mM. Similarly, internal 5HT inhibited I_{Li} at $[K]_{in} = 0$, with maximal efficacy ~50% and IC_{50} ~150 μM (Figs. 6 *B* and 10). Finally, in the absence of internal K, I_{Leak} remains insensitive to internal 5HT (Fig. 6 *C*). Repetition of this experiment with $[K]_{in} = 60$ mM (data not shown) showed that $[5HT]_{in}$ inhibits I_{5HT} at −80 mV, with $IC_{50} = 119 \pm 19\ \mu M$; $[5HT]_{in}$ also inhibits I_{Li}, it but has no effect on I_{Leak}.

Internal Cl weakly affects I_{5HT}, I_{Li}, and I_{Leak}

We observed changes in background currents as $[Cl]_{in}$ was increased or decreased from its normal value (near 50 mM) in both uninjected (data not shown) and injected oocytes, presumably due to endogenous Ca-activated Cl channels (Dascal, 1987; Kuruma and Hartzell, 1999). IOB contains 0.5 mM EGTA, therefore endogenous Cl channel activity and background currents are moderate. We varied $[Cl]_{in}$ from 0 mM to 120 mM by substitution with MES ions. With $[Cl]_{in} = 0$ mM, $5HT_{out}$ activates less I_{5HT} compared to $[Cl]_{in} = 50$ mM (Fig. 7 *A*). In sharp contrast to Na_{in} (Fig. 3 *A*), increasing $[Cl]_{in}$ from 50 mM to 120 mM caused almost no change in I_{5HT} (Fig. 7). I_{Li} (Fig. 7 *B*) and I_{Leak} (Fig. 7 *C*) were little influenced by $[Cl]_{in}$. In addition, $[Cl]_{in}$ had only a small effect on the potency of $5HT_{out}$ on hSERT (Table 1).

DISCUSSION

The COVC technique provides simultaneous access to the internal and external milieu of the oocyte as well as rapid voltage control over a sizable portion (~10%) of the oocyte

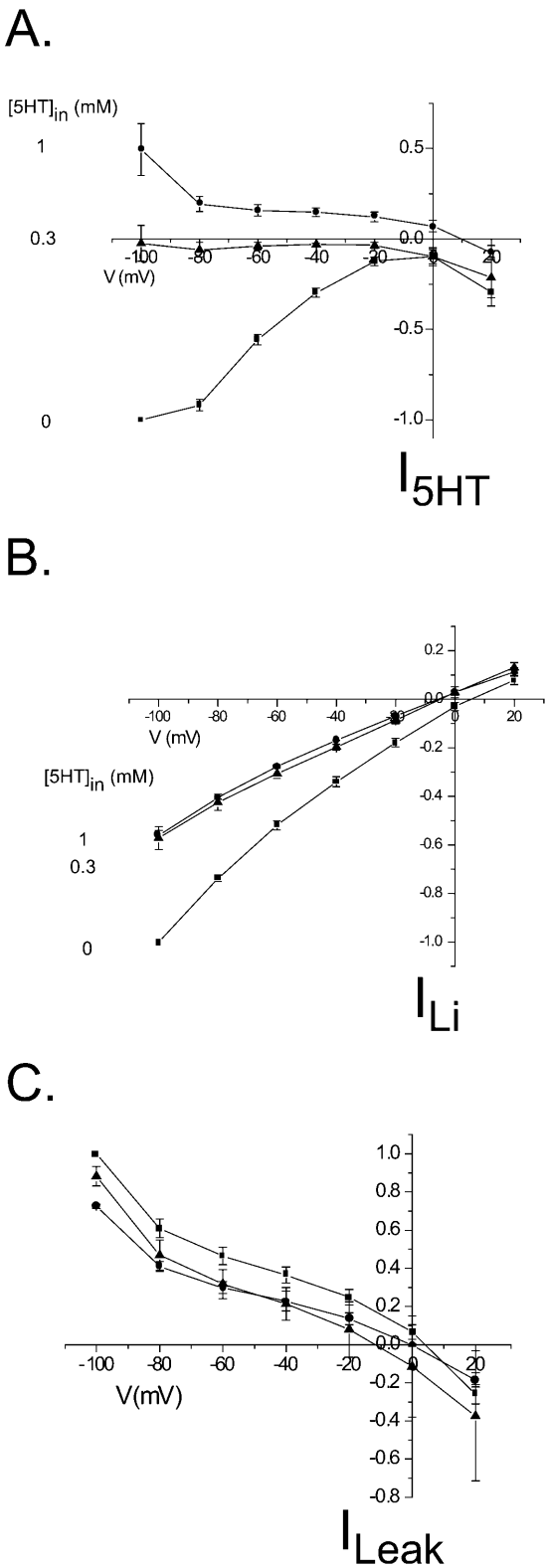

FIGURE 4 Combined effect of elevated $[Na]_{in}$ and $[5HT]_{in}$ on hSERT currents. Steady-state current (Fig. 1) as a function of the test voltage defines $I(V)$ plots. (*A*) $I(V)$ of I_{5HT} ($[5HT]_{out} = 15\ \mu M$), $[5HT]_{in}$ as indicated on figure. (*B*) $I(V)$ of I_{Li}, with changing $[5HT]_{in}$. (*C*) I_{Leak} is insensitive to $[5HT]_{in}$. Symbols in *B* and *C* have the same meaning as in *A*.

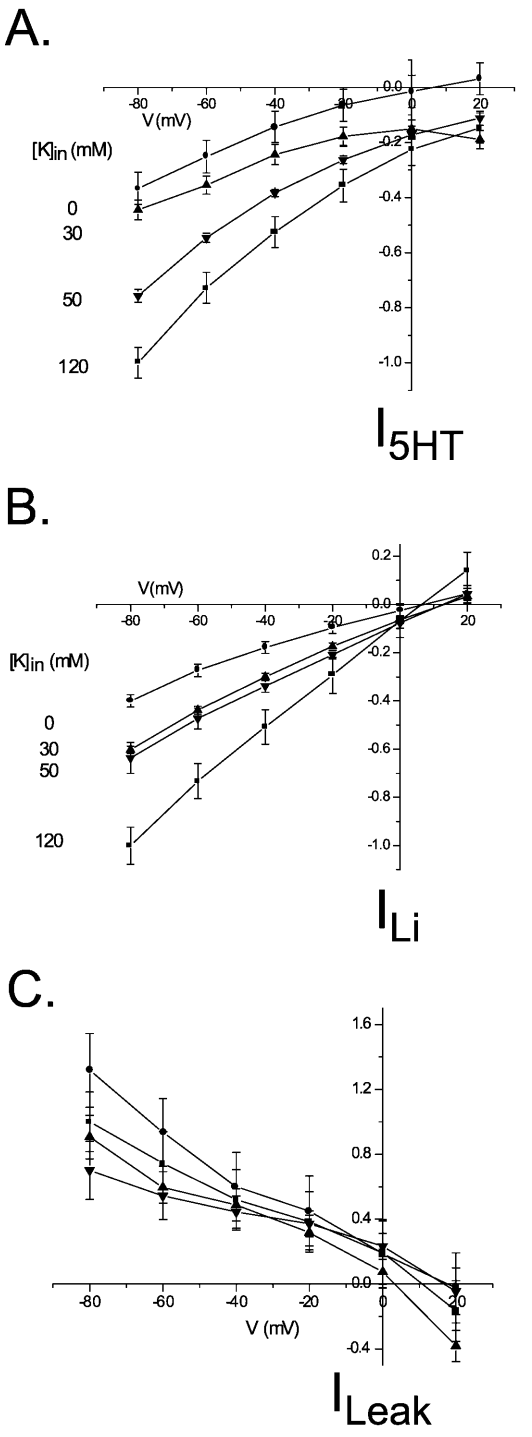

FIGURE 5 Effect of $[K]_{in}$ on hSERT currents. Steady-state current (Fig. 1) as a function of the test voltage defines $I(V)$ plots. (*A*) $I(V)$ of I_{5HT} ($[5HT]_{out} = 15\ \mu M$), $[K]_{in}$ as indicated on figure. (*B*) $I(V)$ of I_{Li}, with changing $[K]_{in}$. (*C*) I_{Leak} is insensitive to $[K]_{in}$. Symbols in *B* and *C* have the same meaning as in *A*.

membrane. As the ionic and voltage conditions facing the hSERT protein are systematically changed, the ionic currents conducted by hSERT are monitored. These ionic currents are ascribed to hSERT because they resemble currents through

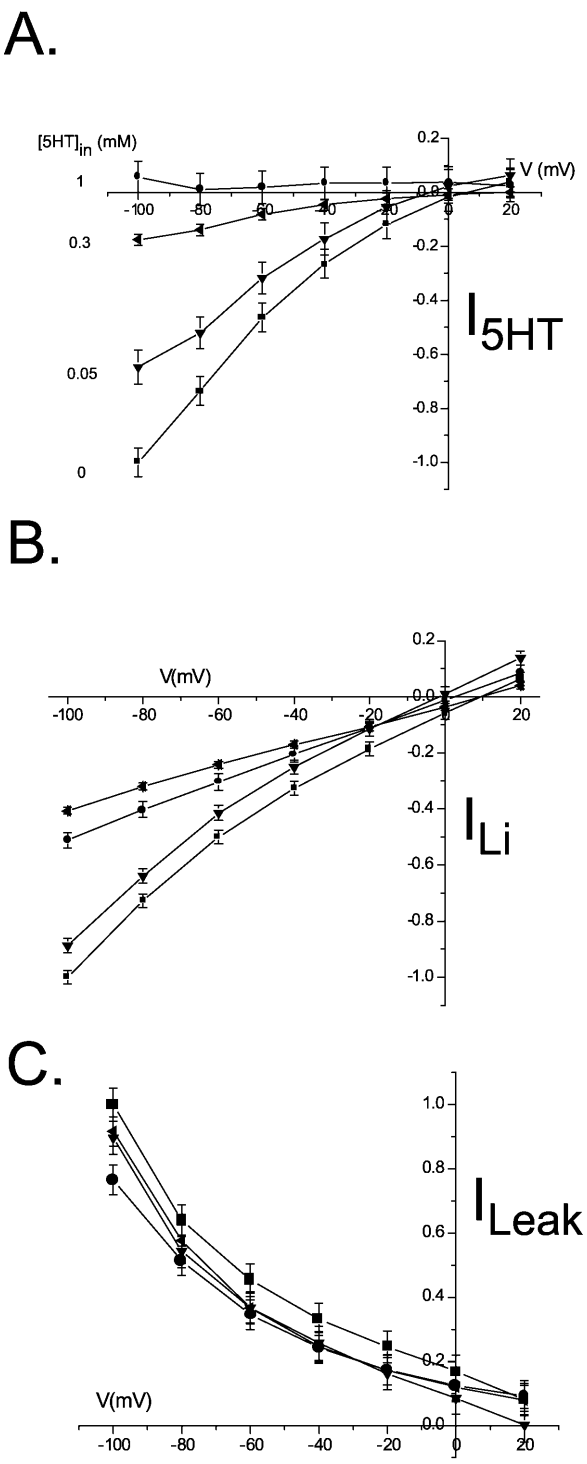

FIGURE 6 Effect of $[5HT]_{in}$ on hSERT currents with $[K]_{in} = 0$. Steady-state current (Fig. 1) as a function of the test voltage defines $I(V)$ plots. (A) $I(V)$ of I_{5HT} ($[5HT]_{out} = 15\ \mu M$), $[5HT]_{in}$ as indicated on figure. (*B*) $I(V)$ of I_{Li}, with changing $[5HT]_{in}$. (*C*) I_{Leak} is insensitive to $[5HT]_{in}$. Symbols in *B* and *C* have the same meaning as in *A*.

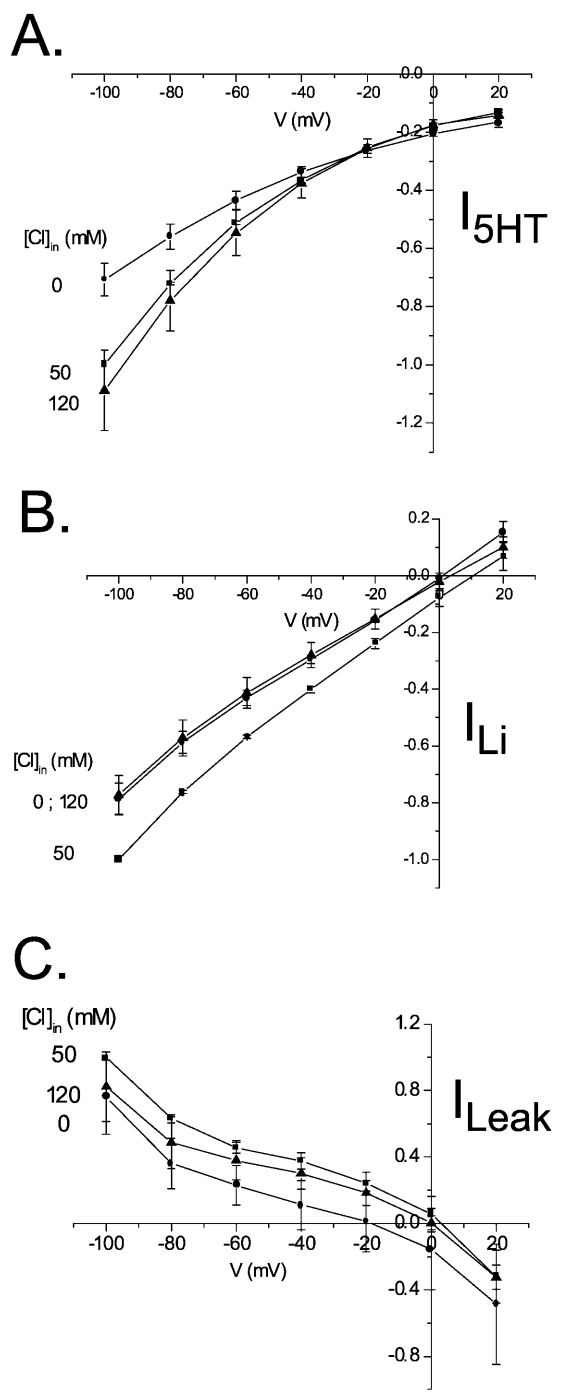

FIGURE 7 Effect of $[Cl]_{in}$ on hSERT currents. Steady-state current (Fig. 1) as a function of the test voltage defines $I(V)$ plots. (A) $I(V)$ of I_{5HT} ($[5HT]_{out} = 15\ \mu M$), $[Cl]_{in}$ as indicated on figure. (*B*) $I(V)$ of I_{Li}, with changing $[Cl]_{in}$. (*C*) I_{Leak} is weakly sensitive to $[Cl]_{in}$. Symbols in *B* and *C* have the same meaning as in *A*.

SERTs (Mager et al., 1994; Galli et al., 1997; Petersen and DeFelice, 1999) and other GAT/NET family members (Mager et al., 1993; Sonders et al., 1997), they are blocked by desipramine, and they present only in oocytes injected with cRNA encoding hSERT.

hSERT conducts several distinct steady-state currents, including substrate-induced current (I_{5HT}), substrate-independent leak current (I_{Leak}), and Li-induced current (I_{Li})

activated by replacement of Na with Li on the external face (in the absence of 5HT). Other currents have also been noted, for example, in acidic (external) pH (Cao et al., 1997). Furthermore, SERTs exhibit transient currents under appropriate conditions (Mager et al., 1994; Li et al., 2002). We have limited our measurements to I_{5HT}, I_{Leak}, and I_{Li} steady-state currents to test prevalent hypotheses about hSERT function.

Because changes in ionic currents result from changes in the fractional occupancy of the conducting conformational states available to hSERT, the sensitivity of I_{5HT}, I_{Leak}, and I_{Li} to various ions will inform our discussion of how the transport of substrate couples to ionic gradients. Thus, a specific model, such as the alternating access model, which postulates distinct relationships between hSERT conformational states, may be rigorously tested.

I_{Leak} insensitivity to internal substrate

hSERT conducts current in the absence of external substrate (Fig. 1 *D*; Mager et al., 1994). This leak current requires external Na, but must permeate a state of hSERT without bound 5HT. Therefore, I_{Leak} may be reasonably assigned to the state $\mathbf{TN_0}$ of Fig. 8 *A*. Measurements of I_{Leak} thus reflect the fractional population of $\mathbf{TN_0}$.

Fig. 2 *C* demonstrates the intriguing result that I_{Leak} is insensitive to internal 5HT. On the basis of a carrier model of SERT function (distinguished by alternating access, such as Fig. 8 *A*), it might be expected that elevation of $[5HT]_{in}$ would draw transporters out of $\mathbf{TN_0}$ and reduce the measured leak. On the other hand, if the dissociation constant for external Na is much smaller than the applied $[Na]_{out}$, the transition $\mathbf{TN_0 \rightarrow T_0}$ would be forbidden. In the absence of external 5HT, transporters could be expected to accumulate in $\mathbf{TN_0}$, and thus be insensitive to the internal milieu. The carrier model can explain the insensitivity of I_{Leak} to $[5HT]_{in}$ by supposing that in the absence of substrate on both sides of the membrane, the molecular rate constants of Fig. 8 *A* dictate that all 5HT binding sites are oriented externally, and hence unavailable to $5HT_{in}$.

Suppression of I_{5HT} by internal 5HT and internal Na

Unlike I_{Leak}, I_{5HT} is suppressed by elevated $[5HT]_{in}$ (Fig. 2 *A*) or $[Na]_{in}$ (Fig. 3 *A*). The alternating access model (Fig. 8 *A*) explains this suppression by inferring that increased $[5HT]_{in}$ or $[Na]_{in}$ leads to sequestration of substrate binding sites on the internal side of the membrane. Therefore elevated $[5HT]_{in}$ or $[Na]_{in}$ results in an reduction in the average number of external binding sites for 5HT, and a concomitant reduction in the current evoked by $5HT_{out}$.

Assuming that SERT conducts I_{5HT} in the state $\mathbf{TNS_0}$, this result implies that the transporters, once in the state $\mathbf{TNS_1}$, release 5HT and Na to the internal milieu more quickly than

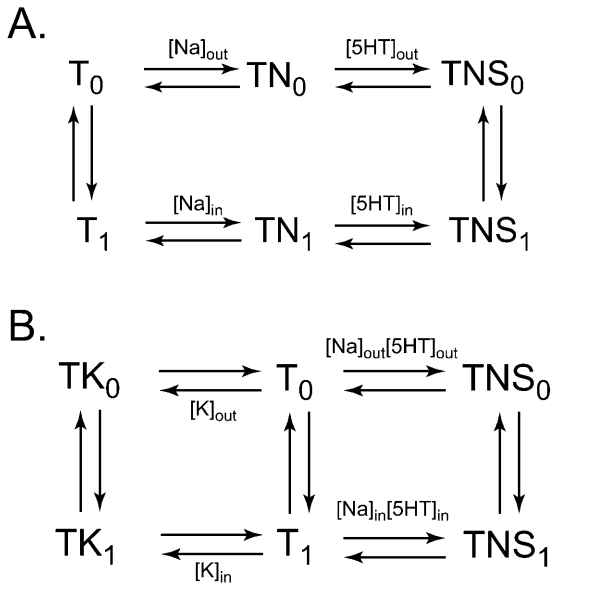

FIGURE 8 The carrier model (distinguished by the alternating access mechanism) used for comparison with voltage-clamp data. (*A*) Alternating access cotransport scheme incorporating ordered binding in which Na (**N**) binds before 5HT (**S**). The state $\mathbf{TS_{out}}$ is assumed to conduct I_{Leak}, whereas $\mathbf{TNS_{out}}$ conducts I_{5HT}. For simplicity, in this diagram the stoichiometric ratio Na:5HT is assumed to be 1:1. (*B*) The alternating access model including nonobligatory K countertransport. Internal K is presumed to stimulate transport when the rate of transition $\mathbf{TK_1 \rightarrow TK_0}$ exceeds the rate $\mathbf{T_1 \rightarrow T_0}$.

they reorient to the outward facing conformation via $\mathbf{TNS_1 \rightarrow TNS_0}$. If SERT reoriented more quickly, $[5HT]_{in}$ would potentiate I_{5HT} since, on average, SERT would spend more time in the state $\mathbf{TNS_0}$. Because elevated $[5HT]_{in}$ or $[Na]_{in}$ decreases the current evoked by external 5HT, a general conclusion is that the rate at which transporters cycle clockwise around Fig. 8 *A* exceeds the rate at which loaded transporters exchange substrate across the membrane.

These data are qualitatively in conflict with a standard result obtained with labeled substrate flux experiments, namely, the phenomenon of transacceleration (Stein, 1986). Previous reports (Sitte et al., 2000, 2001; Adams and DeFelice, 2002) demonstrate that efflux of 5HT through SERT is increased as $[5HT]_{out}$ is increased. This effect is referred to as transacceleration, and within the framework of the carrier model of transport it implies that the rate of equilibrium exchange of substrate is greater than the forward cycling of the transporter (Stein, 1986). That is, for cells loaded with high $[5HT]_{in}$, transacceleration occurs because as $[5HT]_{out}$ increases, the quicker exchange transition $\mathbf{TNS_1 \rightarrow TNS_0}$ dominates over the rate at which transporters proceed from $\mathbf{TNS_1}$ clockwise around the transport cycle (Fig. 8 *A*). Thus, if transacceleration measurements (Sitte et al., 2000, 2001; Adams and DeFelice, 2002) are accurate and correctly interpreted within the prevailing carrier model (Fig. 8 *A*), elevated $[5HT]_{in}$ would increase I_{5HT}, because inward-facing transporters ($\mathbf{TNS_1}$) would quickly reorient to

the conducting state ($\mathbf{TNS_0}$). This expectation is, however, opposite to the electrophysiological measurements (Fig. 2 *A*).

In addition, if the carrier model is evoked to explain the suppression of I_{5HT} by assuming that transporters reorient toward the internal face when $[5HT]_{in}$ or $[Na]_{in}$ is elevated, then the result displayed in Fig. 4 *A* is inexplicable. In this experiment, both $[Na]_{in}$ and $[5HT]_{in}$ are elevated. According to the carrier model, suppression of I_{5HT} under these conditions indicates that the transporters are facing inward. However, Fig. 4 *A* shows that application of external 5HT still interacts with SERT to effectively block I_{Leak}, implying that many transporters still have external binding sites. Thus a carrier model in which the suppression of I_{5HT} by internal 5HT (Fig. 2 *A*) or Na (Fig. 3 *A*) is predicted cannot also predict the result shown in Fig. 4 *A*.

The carrier model (Fig. 8 *A*) is unable to consistently explain the electrophysiological data (Figs. 2 *A*, 3 *A*, and 4 *A*) and the body of transacceleration data (Sitte et al., 2000, 2001; Adams and DeFelice, 2002). Instead, we speculate that there may be distinct internal and external modes of interaction between hSERT and 5HT. Transacceleration can be explained by a functional model in which external 5HT binds to an external site and opens a pore through hSERT, increasing the rate of efflux through the pore in apparent contradiction to the driving force. The large suppression of I_{5HT} by internal 5HT might not be entirely explained by a straightforward reduction in the driving force for inward 5HT permeation through the pore, because it has been demonstrated that permeating 5HT itself carries, at most, 15% of the measured I_{5HT} (Galli et al., 1997).

However, in a complex, single-file pore, the suppression of current by internal 5HT can be nonlinearly related to the reduction in the driving gradient. Thus, 5HT may in effect occlude the pore for I_{5HT} (Fig. 2 *A*). Likewise, the suppression of I_{5HT} by $[Na]_{in}$ elevation (Fig. 3 *A*) may result from decreased driving force for net inward Na permeation through a complex pore. External Li activates a pore, which does not support transport of 5HT, but internal 5HT can enter and block the pore (Fig. 2 *B*). Additional conformational changes in hSERT may also be necessary to explain the increase in external 5HT potency in the presence of internal 5HT (Table 1).

Internal K does not compete with internal 5HT for internal hSERT binding sites

The idea that hSERT countertransports K, with respect to 5HT, rests on the observation that elevated $[K]_{in}$ increases the rate of 5HT transport (Rudnick and Nelson, 1978; Nelson and Rudnick, 1979). This has been incorporated into the alternating access model by supposing that internal K accelerates the rate at which internally facing 5HT-binding sites reface to the external orientation (Rudnick and Nelson, 1978; Fig. 8 *B*). We therefore sought to test how changing $[K]_{in}$ affects hSERT currents (Fig. 5). Consistent with the transport data, these experiments reveal that increasing $[K]_{in}$ increases I_{5HT}, suggesting a larger average number of available external 5HT binding sites when $[K]_{in}$ is elevated. Furthermore, we also observe a decrease in external 5HT potency with increased $[K]_{in}$ (Table 1), as predicted by the countertransport hypothesis (Fig. 8 *B*; Nelson and Rudnick, 1979).

Therefore we combined the experiments of Figs. 2 and 5, to study directly the interaction between internal K and internal 5HT at hSERT. Fig. 6 shows that K_{in} is not required for $5HT_{in}$ to suppress I_{5HT}, and we also found that internal K does not change the potency with which internal 5HT suppresses I_{5HT}. In the specific K countertransport model proposed previously (Fig. 8 *B*; Nelson and Rudnick, 1979), internal 5HT and K compete for internally facing, empty transporters. If this were the case, we expect that the potency of 5HT would decrease with increasing $[K]_{in}$, counter to our observations. Proton (H) substitution for K on the internal face of hSERT does not effect our results since at our experimental $pH_{in} = pH_{out} = 7.4$, proton stimulation of 5HT transport through SERT is negligible even in the absence of K (Keyes and Rudnick, 1982).

Furthermore, Fig. 5 *B* demonstrates that internal K acts to potentiate I_{Li} as well as I_{5HT}. Since I_{Li} cannot be associated with a transport-competent mode of hSERT (Ni et al., 2001; Petersen and DeFelice, 1999), the hypothesis that K_{in} acts to accelerate refacing of the transporter does not apply.

To explain the acceleration of transport by K (Nelson and Rudnick, 1979) and the reduction of I_{5HT} and I_{Li} by removal of K_{in} (Fig. 5, *A* and *B*), we postulate that internal K interacts with hSERT at a modulatory site, which is available only when 5HT or Li is bound to their external sites. The mechanism of K modulation could be that K acts to stabilize the open states of the 5HT-activated and Li-activated hSERT pore. In contrast, the internal K site is unavailable when hSERT is in the leakage state.

Na and Cl affect hSERT differentially

Although the putative transport cycle of hSERT cotransports one Na and one Cl (Rudnick and Clark, 1993) we observe that these ions have opposite effects on I_{5HT} from the internal face of the transporter (Figs. 3 *A* and 7 *A*). If the reduction in I_{5HT} by internal Na were due to sequestration of the binding site to the internal face of the membrane, it is difficult to see how the other co-ion, Cl, could have an opposite effect. GAT1 current is reported to display the opposite behavior with respect to internal Cl (Lu and Hilgemann, 1999). In that case, the measured suppression of GABA-induced current through GAT1 by internal Cl was interpreted as evidence that Cl facilitates the release of GABA from the internally facing transporter substrate site, after cotransport of GABA and Cl (Hilgemann and Lu, 1999). Clearly, such a role for Cl in hSERT is not supported by our data. Rather, Cl^- likely plays a regulatory role in hSERT function. In support of our

interpretation, Loo et al. (2000) report that Cl is exchanged in GAT1 and uncoupled to substrate transport, and Cl does not contribute to net transported charge.

As we have argued for K, it is possible that Cl may bind hSERT and influence the relative permeability of 5HT and Na. This would alter the magnitude and pharmacology of the observed I_{5HT}, and could make it appear that Cl ions are coupled to 5HT transport. Our data (Fig. 7 *A*) are consistent with Cl permeation contributing to I_{5HT}, but a previous report strongly argues against this possibility (Lin et al., 1996). In any case, we cannot conceive a way in which both Cl and Na are cotransported with 5HT, yet have opposite effects on I_{5HT}, within the prevailing alternating access models.

I_{5HT}, I_{Leak}, and I_{Li} are distinct conducting states of hSERT

hSERT conducts multiple ionic currents in addition to the substrate-gated current I_{5HT}. Previous work (Mager et al., 1994; Sonders et al., 1997; Petersen and DeFelice, 1999; and Fig. 4 *A*) shows that whereas I_{5HT} is activated by external 5HT, I_{Leak} is blocked. Thus these two conduction states of hSERT are mutually exclusive if, by definition, a single hSERT cannot simultaneously conduct I_{Leak} and I_{5HT}. This suggests that I_{5HT} and I_{Leak} are different states of a single pore with different conduction properties. Unitary currents for I_{5HT} and I_{Leak} (Lin et al., 1996) support this conclusion.

Our data are consistent with this idea but add significant details. Although I_{5HT} and I_{Leak} may share a pathway, Fig. 2 *C* demonstrates that only external 5HT acts to shift the pathway into the I_{5HT} mode. Internal 5HT alone, in the absence of external 5HT, does not appear to alter the hSERT channel or permeate hSERT, because, if it did so, then the current blocked by external desipramine would be altered. Previous work (Mager et al., 1994; Lin et al., 1996; Petersen and DeFelice, 1999) suggested that Na permeation contributes to I_{Leak}, because I_{Leak} requires external Na. Fig. 3 *C* demonstrates that elevating $[Na]_{in}$ shifts the reversal potential of I_{Leak} to more negative values, strengthening the conclusion that Na permeates hSERT in the leak state.

A puzzling aspect of our data is that the reversal potential of I_{Leak} shifts through 0, indicating that other ions contributing to I_{Leak} have negative reversal potentials, for example, K (−100 mV) and Cl (−20 mV) under these experimental conditions. Yet Fig. 5 *C* suggests that K does not contribute to I_{Leak}. Fig. 7 *C* indicates that Cl may contribute to I_{Leak}, as evidenced by a small apparent shift in the reversal potential to negative values in the absence of internal Cl. In contrast, previous work (Lin et al., 1996) demonstrates that Cl is not a major contributor to hSERT mediated currents. Of the ions thought to permeate hSERT, this leaves only H (Cao et al., 1997) to carry the leak current with Na. However, because we always fix internal and external pH to 7.4, the reversal potential for H should be 0. Thus, we are unable to state unequivocally which ions constitute the leak current in addition to Na.

Finally, for each set of experimental conditions we substituted all of the external Na with Li, which is known to activate a large current through hSERT (Mager et al., 1994; Petersen and DeFelice, 1999; Ni et al., 2001). Petersen and DeFelice (1999) employed two-electrode voltage clamp to study the interaction between Li and Na at the external face of the *Drosophila* SERT, and concluded that they compete within a shared permeation pathway. On the other hand, Ni et al. (2001) inferred from a combination of biochemical and electrophysiological data that Li induces a conformational change in SERT, opening a conduction pore, and that this conformational change is blocked by Na. Our data support the later view, since we observe that internal 5HT can distinguish between I_{Leak} and I_{Li} (Fig. 2) and that elevated $[Na]_{in}$ has no effect upon I_{Li} (Fig. 3 *B*). Together these results argue that the channel induced by external Li is not permeable to Na, and that competition between Na and Li occurs completely on the external face of the transporter, rather than within a transmembrane pore.

We conclude from the electrophysiological data that I_{5HT}, I_{Li}, and I_{Leak} are separate conducting states of hSERT, because $5HT_{in}$, K_{in}, and Na_{in} can effectively discriminate these states. We favor the idea that these states represent different permeability and selectivity states of the same physical permeation pathway, since this easily explains why the states are mutually exclusive. However, we cannot completely rule out a set of distinct pathways allosterically linked in a complex manner.

SUMMARY

We have investigated the conduction states of hSERT under a variety of ionic conditions. Our data indicate serious flaws in the hypothesis of alternating access as a mechanism of gradient coupling. This hypothesis does not consistently explain transport and electrophysiological data. We are able to isolate simultaneously distinct external and internal binding sites for substrate, which exert different effects upon currents conducted by hSERT, in contradiction to the alternating access model. We also infer that the external binding site of the coupled ion Na is likewise simultaneously accessible from the internal and external face, if we assume that Li and Na share an external binding site. Although Na and Cl are putatively cotransported, they have opposite effects on the internal face of the transporter. Although K plays a complex role in hSERT function, it does not compete with the substrate for empty internal transporters.

We find the qualitative discrepancies between our data and the expectations of the alternating access hypothesis compelling. We therefore propose that much of the behavior of hSERT can be explained in the language of ion channels, rather than a carrier model employing an alternating access mechanism. I_{5HT}, I_{Li}, and I_{leak} represent different conducting

states of hSERT, most likely different states of the same physical permeation route through the protein. This naturally explains the inhibition by internal 5HT and the competition between Na and Li at the external face of hSERT. We hypothesize that I_{5HT} represents the transport mode of hSERT, in which 5HT and Na couple in a shared pore, gated by external 5HT and modulated by K and Cl.

The authors thank Hongping Yuan for technical assistance and oocyte culture, and Dr. F. Bezanilla and Dr. D. Starace (UCLA) for generous help with the cut-open oocyte technique.

This research was supported by National Institutes of Health grant RO1 NS-34075.

REFERENCES

Adams, S. V., and L. J. DeFelice. 2002. Flux coupling in the human serotonin transporter. *Biophys. J.* 83:3268–3282.

Blakely, R. D., L. J. DeFelice, and H. C. Hartzell. 1994. Molecular physiology of norepinephrine and serotonin transporters. *J. Exp. Biol.* 196:263–281.

Bunin, M. A., and R. M. Wightman. 1998. Quantitative evaluation of 5-hydroxytryptamine (serotonin) neuronal release and uptake: an investigation of extrasynaptic transmission. *J. Neurosci.* 18:4854–4860.

Cao, Y., M. Li, S. Mager, and H. A. Lester. 1998. Amino acid residues that control pH modulation of transport-associated current in mammalian serotonin transporters. *J. Neurosci.* 18:7739–7749.

Cao, Y., S. Mager, and H. A. Lester. 1997. H^+ permeation and pH regulation at a mammalian serotonin transporter. *J. Neurosci.* 17:2257–2266.

Chen, X. Z., M. J. Coady, F. Jackson, A. Berteloot, and J. Y. Lapointe. 1995. Thermodynamic determination of the Na+: glucose coupling ratio for the human SGLT1 cotransporter. *Biophys. J.* 69:2405–2414.

Chen, X. Z., M. J. Coady, and J. Y. Lapointe. 1996. Fast voltage clamp discloses a new component of presteady-state currents from the Na(+)-glucose cotransporter. *Biophys. J.* 71:2544–2552.

Chen, J. J., Z. Li, H. Pan, D. L. Murphy, H. Tamir, H. Koepsell, and M. D. Gershon. 2001. Maintenance of serotonin in the intestinal mucosa and ganglia of mice that lack the serotonin transporter: abnormal intestinal motility and the expression of cation transporters. *J. Neurosci.* 21:6348–6361.

Chou, T. 1999. Kinetics and thermodynamics across single-file pores: solute permeability and rectified osmosis. *J. Chem. Phys.* 110:606–615.

Chou, T., and D. Lohse. 1999. Entropy-driven pumping in zeolites and biological membranes. *Phys. Rev. Lett.* 82:3552–3555.

Coady, M. J., X. Z. Chen, and J. Y. Lapointe. 1996. rBAT is an amino acid exchanger with variable stoichiometry. *J. Membr. Biol.* 149:1–8.

Coady, M. J., F. Jalal, X. Chen, G. Lemay, A. Berteloot, and J. Y. Lapointe. 1994. Electrogenic amino acid exchange via the rBAT transporter. *FEBS Lett.* 356:174–178.

Costa, A. C., J. W. Patrick, and J. A. Dani. 1994. Improved technique for studying ion channels expressed in Xenopus oocytes, including fast superfusion. *Biophys. J.* 67:395–401.

Dascal, N. 1987. The use of *Xenopus* oocytes for the study of ion channels. *CRC. Crit. Rev. Biochem.* 22:317–387.

DeFelice, L. J., and S. V. Adams. 2001. Serotonin and norepinephrine transporters: possible relationship between oligomeric structure and channel modes of conduction. *Molecl. Memb. Biology.* 18:45–51.

DeFelice, L. J., S. V. Adams, and D. Ypey. 2001. Single-file diffusion and neurotransmitter transporters: Hodgkin's mechanical model revisited. *Biosystems.* 62:57–66.

Eddahibi, S., M. Humbert, E. Fadel, B. Raffestin, M. Darmon, F. Capron, G. Simmmoneau, P. Dartevelle, M. Hamon, and S. Adnot. 2001. Serotonin transporter overexpression is responsible for pulmonary artery smooth muscle hyperplasia in primary pulmonary hypertension. *J. Clin. Invest.* 108:1141–1150.

Elsner, H.-A., H.-H. Honck, F. Willmann, H.-J. Kreienkamp, and F. Iglauer. 2000. Poor quality of oocytes from Xenopus laevis used in laboratory experiments: prevention by use of antiseptic surgical technique and antibiotic supplementation. *Comp. Med.* 50:206–211.

Galli, A., R. D. Blakely, and L. J. DeFelice. 1996. Norepinephrine transporters have channel modes of conduction. *Proc. Natl. Acad. Sci. USA.* 93:8671–8676.

Galli, A., R. D. Blakely, and L. J. DeFelice. 1998. Patch-clamp and amperometric recordings from norepinephrine transporters: channel activity and voltage-dependent uptake. *Proc. Natl. Acad. Sci. USA.* 95:13260–13265.

Galli, A., C. I. Petersen, M. deBlaquiere, R. D. Blakely, and L. J. DeFelice. 1997. *Drosophila* serotonin transporters have voltage-dependent uptake coupled to a serotonin-gated ion channel. *J. Neurosci.* 17:3401–3411.

Goldin, A. L. 1992. Maintenance of *Xenopus laevis* and oocyte injection. *Methods Enzymol.* 207:266–279.

Gu, H., S. C. Wall, and G. Rudnick. 1994. Stable expression of biogenic amine transporters reveals differences in inhibitor sensitivity, kinetics, and ion dependence. *J. Biol. Chem.* 269:7124–7130.

Gu, H., S. C. Wall, and G. Rudnick. 1996. Ion coupling stoichiometry for the norepinephrine transporter in membrane vesicles from stably transfected cells. *J. Biol. Chem.* 271:6911–6916.

Hilgemann, D. W., and C. C. Lu. 1999. GAT1 (GABA:Na+:Cl−) cotransport function. Database reconstruction with an alternating access model. *J. Gen. Physiol.* 114:459–475.

Hodgkin, A. L., and R. D. Keynes. 1955. The potassium permeability of a giant nerve fibre. *J. Physiol.* 128:61–88.

Ingram, S. L., and S. G. Amara. 2000. Arachidonic acid stimulates a novel cocaine-sensitive cation conductance associated with the human dopamine transporter. *J. Neurosci.* 20:550–557.

Iversen, L. L. 1971. Role of transmitter uptake mechanisms in synaptic neurotransmission. *Br. J. Pharmacol.* 41:571–591.

Jardetsky, O. 1966. Simple allosteric model for membrane pumps. *Nature.* 211:969–970.

Kaneko, S., A. Akaike, and M. Satoh. 1998. Cut-open recording techniques. *Methods Enzymol.* 293:319–331.

Keyes, S. R., and G. Rudnick. 1982. Coupling of transmembrane proton gradients to platelet serotonin transport. *J. Biol. Chem.* 257:1172–1176.

Kuruma, A., and H. C. Hartzell. 1999. Dynamics of calcium regulation of chloride currents in *Xenopus* oocytes. *Am. J. Physiol.* 276:C161–C175.

Läuger, P. 1991. Electrogenic Ion Pumps. Sinauer Associates, Sunderland, MA.

Li, M., R. A. Farley, and H. A. Lester. 2002. Voltage-dependent transient currents of human and rat 5-HT transporters (SERT) are blocked by HEPES and ion channel ligands. *FEBS Lett.* 513:247–252.

Lin, F., H. A. Lester, and S. Mager. 1996. Single-channel currents produced by the serotonin transporter and analysis of a mutation affecting ion permeation. *Biophys. J.* 71:3126–3135.

Loo, D. D. F., S. Eskandari, K. J. Boorer, H. K. Sarkar, and E. M. Wright. 2000. Role of Cl− in electrogenic Na+-coupled cotransporters GAT1 and SGLT1. *J. Biol. Chem.* 275:37414–37422.

Lu, C.-C., and D. Hilgemann. 1999. GAT1 (GABA:Na:Cl) cotransport function. *J. Gen. Physiol.* 114:429–444.

Mager, S., C. Min, D. J. Henry, C. Chavkin, B. J. Hoffman, N. Davidson, and H. A. Lester. 1994. Conducting states of a mammalian serotonin transporter. *Neuron.* 12:845–859.

Mager, S., J. Naeve, M. Quick, C. Labarca, N. Davidson, and H. A. Lester. 1993. Steady states, charge movements, and rates for a cloned GABA transporter expressed in Xenopus oocytes. *Neuron.* 10:177–188.

Nelson, P. J., and G. Rudnick. 1979. Coupling between platelet 5-hydroxytryptamine and potassium transport. *J. Biol. Chem.* 254:10084–10089.

Ni, Y. G., J. G. Chen, A. Androutsellis-Theotokis, C. J. Huang, E. Moczydlowski, and G. Rudnick. 2001. A lithium-induced conformational change in serotonin transporter alters cocaine binding, ion conductance, and reactivity of Cys-109. *J. Biol. Chem.* 276:30942–30947.

Petersen, C. I., and L. J. DeFelice. 1999. Ionic interactions in the *Drosophila* serotonin transporter identify it as a serotonin channel. *Nat. Neurosci.* 2:605–610.

Quick, M. W., J. Naeve, N. Davidson, and H. A. Lester. 1992. Incubation with horse serum increases viability and decreases background neurotransmitter uptake in Xenopus oocytes. *Biotechniques.* 13:357–361.

Ramamoorthy, S., A. L. Bauman, K. R. Moore, H. Han, T. Yang-Feng, A. S. Chang, V. Ganapathy, and R. D. Blakely. 1993. Antidepressant- and cocaine-sensitive human serotonin transporter: molecular cloning, expression, and chromosomal localization. *Proc. Natl. Acad. Sci. USA.* 90:2542–2546.

Ramsey, I. S., and L. J. DeFelice. 2002. Serotonin transporter function and pharmacology are sensitive to expression level: evidence for an endogenous regulatory factor. *J. Biol. Chem.* 277:14475–14482.

Rudnick, G. 1977. Active transport of 5-hydroxytryptamine by plasma membrane vesicles isolated from human blood platelets. *J. Biol. Chem.* 252:2170–2174.

Rudnick, G. 1998. Ion-coupled neurotransmitter transport: thermodynamic vs. kinetic determinations of stoichiometry. *Methods Enzymol.* 296:233–247.

Rudnick, G., and J. Clark. 1993. From synapse to vesicle: the reuptake and storage of biogenic amine neurotransmitters. *Biochim. Biophys. Acta.* 1144:249–263.

Rudnick, G., and P. J. Nelson. 1978. Platelet 5-hydroxytryptamine transport, an electroneutral mechanism coupled to potassium. *Biochem.* 17:4739–4742.

Sitte, H. H., B. Hiptmair, J. Zwach, C. Pifl, E. A. Singer, and P. Scholze. 2001. Quantitative analysis of inward and outward transport rate in cells stably expressing the cloned human serotonin transporter: inconsistencies with the hypothesis of facilitated transport. *Molecl. Pharmacol.* 59:1129–1137.

Sitte, H. H., P. Scholze, P. Schloss, C. Pifl, and E. A. Singer. 2000. Characterization of carrier-mediated efflux in human embryonic kidney 293 cells stably expressing the rat serotonin transporter: a superfusion study. *J. Neurochem.* 74:1317–1324.

Sonders, M. S., and S. G. Amara. 1996. Channels in transporters. *Curr. Opin. Neurobiol.* 6:294–302.

Sonders, M. S., S. J. Zhu, N. R. Zahniser, M. P. Kavanaugh, and S. G. Amara. 1997. Multiple ionic conductances of the human dopamine transporter: the actions of dopamine and psychostimulants. *J. Neurosci.* 17:960–974.

Stefani, E., and F. Bezanilla. 1998. Cut-open oocyte voltage-clamp technique. *Methods Enzymol.* 293:300–318.

Stein, W. D. 1986. Transport and Diffusion Across Cell Membranes. Academic Press, New York.

Stuhmer, W. 1998. Electrophysiologic recordings from *Xenopus* oocytes. *Methods Enzymol.* 293:280–300.